Optimization of the Expression, Purification, and Crystallization of SARS-CoV-2 Nonstructural Protein 13

Optimization of the Expression, Purification, and Crystallization of SARS-CoV-2 Nonstructural Protein 13

by

Teri Tran

Under the Direction of Ming Luo, PhD

A Thesis Submitted in Partial Fulfillment of the Requirements for the Degree of

Master of Science

in the College of Arts and Sciences

Georgia State University

2025

ABSTRACT

The SARS-CoV-2 nonstructural protein 13 (nsp13) is a helicase essential for viral replication, making it a promising antiviral target. The goal of this study is to optimize the expression, purification, and crystallization of recombinant nsp13. An *Escherichia coli* host was transformed with a plasmid containing an N-terminal His6-Zb-TEV-tagged nsp13 gene. Expression of nsp13 protein was then induced in the transformed bacteria. Protein purification involved immobilized metal affinity chromatography, ion-exchange chromatography, and size exclusion chromatography. SDS-PAGE confirmed successful purification, showing a distinct band at the expected molecular weight. TEV protease cleavage removed the His6-Zb tag, followed by further purification to obtain pure cleaved nsp13. The resulting high-purity nsp13 was suitable for crystallization trials. This study presents a reproducible protocol for the efficient expression and purification of nsp13, facilitating the way for structural characterization. Successful production of pure nsp13 protein lays the foundation for future biochemical studies to identify helicase-targeting inhibitors.

INDEX WORDS: Nsp13, Recombinant protein, Expression, Purification, Crystallization, Biochemistry

Optimization of the Expression, Purification, and Crystallization of SARS-CoV-2 Nonstructural Protein 13

by

Teri Tran

Committee Chair: Ming Luo

Committee: Jenny Yang

Bingchen Yu

Electronic Version Approved:

Office of Graduate Services

College of Arts and Sciences

Georgia State University

May 2025

DEDICATION

I dedicate this thesis to my love, Gabriel, whose unwavering support and encouragement have meant everything to me. I also dedicate this work to my family who have given me so much support: to my mom and dad, for their hard work and sacrifices helping me grow up, and to my two younger sisters, whose strength, belief, and support have carried me through the toughest times.

ACKNOWLEDGEMENTS

I want to give many thanks to the members of my lab who have supported and guided me throughout my academic journey. Their mentorship, collaboration, and encouragement have been important to both my personal and professional growth. I am especially thankful to Scarlet Tang, who took the time to teach me the essential techniques for protein expression, purification, and crystallization. Her patience and attention to detail laid the foundation for much of the experimental work presented in this thesis. I would also like to thank Foyin Faniyi, who started in the lab around the same time as I did, and has always offered me valuable guidance and support to help refine my laboratory skills. She has generously shared her knowledge, provided thoughtful advice, and helped me troubleshoot challenges in my experiments. Her spirit for teamwork and willingness to teach the skills she developed have made a difference in my growth as a researcher. I want to thank Kristin Van Mouwerik Lyles because she is an amazing mentor. Her ability to clearly explain complex scientific concepts and her readiness to answer my many questions with kindness and depth made a lasting impact on my learning experience. I am also grateful to Edwin Ogbonna for his assistance with my protein purification and crystallization work. His collaboration and hardwork have made these challenging processes much more manageable.

I would also like to express my deepest gratitude to thank my professors at Georgia State University. I want to thank Dr. Gigi Ray, whose encouragement played a big role in my decision to join a research lab. Her outstanding academic and professional guidance made me into a more confident student. Also, her skills as a biochemistry lecturer created a strong foundation for my basic knowledge of biochemistry, I would also like to thank my thesis committee members, Dr. Jenny Yang and Dr. Bingchen Ye, for their time, insight, and valuable contributions to this work.

Their thoughtful feedback and expert guidance were important in shaping and refining this thesis. I am deeply appreciative of the knowledge they shared and the support they provided throughout this process. Lastly, and certainly not least, my deepest appreciation goes to Dr. Ming Luo for giving me the opportunity to join his lab as an undergraduate student. I am thankful for his mentorship in teaching me essential laboratory techniques and for welcoming me to continue my research in his lab throughout my master's program. Dr. Luo's expertise in protein expression, purification, and crystallization has greatly influenced my academic and scientific growth. His insightful feedback, thoughtful suggestions, and high standards have consistently pushed me to improve the quality of my experiments and to think critically as a researcher. His trust and support have been fundamental to my growth as a researcher, and I am honored to have been a part of his team.

TABLE OF CONTENTS

LIST OF FIGURES

1 INTRODUCTION

1.1 Recombinant Protein Expression and Purification

1.1.1. Recombinant Protein Expression

Recombinant protein expression is a fundamental technique in molecular biology and biotechnology that enables the production of specific proteins in a controlled environment. By using recombinant DNA technology, a gene encoding the protein of interest is inserted into an expression vector (also known as a plasmid), which is then introduced into a suitable host cell. The choice of the host system, such as *Escherichia coli*, yeast, insect, or mammalian cells, depends on factors like protein solubility, yield, and the need for post-translational modifications.[1]

The process begins with vector construction, where regulatory elements such as promoters, ribosome-binding sites, and selection markers are incorporated to ensure efficient transcription and translation (Figure 1).[1] Once introduced into the host cell, protein expression can be induced under optimized conditions, including temperature, inducer concentration, and growth media composition.[2] However, challenges such as protein misfolding, inclusion body formation, and toxicity to the host cell must be addressed through strategies like co-expression of chaperones or modifying expression parameters.[2]

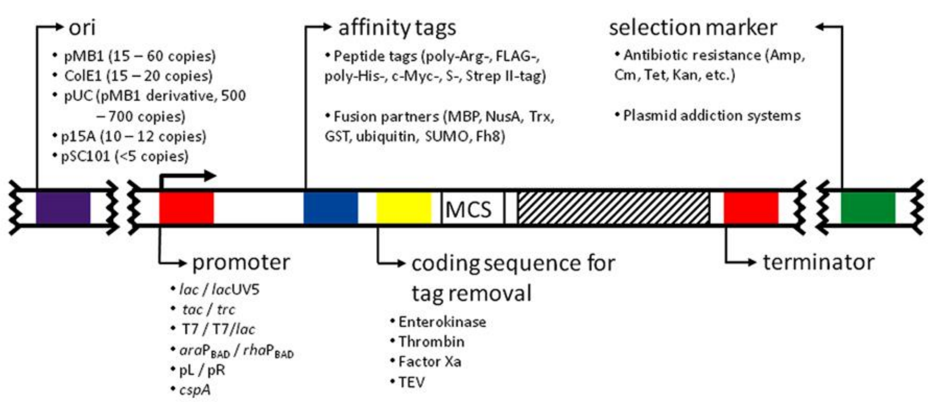

Figure 1. Layout of an expression vector, highlighting the main features.[1]

1.1.2. Recombinant Proteins with His-tag

One of the most widely employed techniques for protein purification is the use of His-tag technology, which involves adding a short polyhistidine sequence (usually six histidine residues) to the target protein (Figure 2).[3] The His-tag provides several advantages in recombinant protein purification. Its small size and minimal impact on the protein's structure and function make it an ideal tool for protein isolation, especially for proteins that need to remain active or stable during purification.[4] The process is also highly versatile, as the His-tag can be added to either the N-terminus or C-terminus of the recombinant protein, and in some cases, it can even be placed within the protein itself without disrupting its functional properties.[5]

Figure 2. Layout of how an affinity tag is attached to a target protein.[5]

His-tag purification is widely used in various applications, ranging from structural studies, where large quantities of pure protein are required for techniques like X-ray crystallography or NMR spectroscopy, to the production of therapeutic proteins, enzymes, or antibodies.[4] Furthermore, the His-tag method can be employed in combination with other affinity tags or chromatographic techniques to further enhance purity or allow for additional functional characterizations.[3] Given its simplicity, efficiency, and adaptability, recombinant protein expression with His-tag technology has become a fundamental aspect of modern protein biochemistry and biotechnology.

To make sure the recombinant protein is functional, the His-tag is often cleaved off after purification using site-specific proteases such as Tobacco Etch Virus (TEV) protease. TEV protease is highly specific, recognizing the amino acid sequence (ENLYFQ/S or G) and cleaving between glutamine and serine or glycine.[6] This allows for the removal of the His-tag without leaving extra residues that could interfere with downstream applications. TEV protease is useful when native or functional proteins are required for structural studies, enzymatic assays, or therapeutic applications. Additionally, TEV protease is often co-expressed with the target protein or immobilized on a resin for controlled cleavage, minimizing unwanted side reactions and ensuring efficient tag removal.[6] Its high specificity and efficiency make TEV protease a valuable tool in recombinant protein preparation.

1.1.3. Affinity Chromatography

Affinity chromatography is a highly efficient and selective technique used for the purification of proteins based on their specific binding interactions with a ligand immobilized on a stationary phase. This technique takes advantage on the natural or engineered affinity between a target molecule and a ligand, making it an indispensable tool in molecular biology, biochemistry, and biotechnology.[7] Affinity chromatography is widely used to isolate recombinant proteins, particularly when they are fused to affinity tags such as the polyhistidine (His) tag. The His-tag is commonly incorporated into recombinant proteins to facilitate their purification.

In the case of His-tagged proteins, affinity chromatography uses immobilized metal affinity chromatography (IMAC), where the stationary phase is functionalized with metal ions, such as nickel (Ni^{2+}), cobalt (Co^{2+}), or copper (Cu^{2+}), that specifically bind to the histidine residues of the His-tag.[8] When a sample containing His-tagged proteins is passed through the chromatography column, the His-tagged protein binds to the metal ions, while other non-target proteins and contaminants are washed away.[9] The interaction between the histidine residues and the metal ions is typically strong, but can be competitively displaced by the introduction of an imidazole solution, which has a similar structure to histidine and competes for binding sites on the metal ions.[9] This allows for the selective elution of the His-tagged protein from the column, often resulting in high purity with minimal need for additional purification steps. One of the key advantages of using His-tag affinity chromatography is its simplicity and speed. The process can be performed in a single step, making it highly efficient for isolating proteins, particularly when large-scale production is required.[5]

The high specificity and minimal loss of biological activity during the purification process makes it valuable for experiments that require high-quality, active protein. Furthermore, His-tag affinity chromatography can be coupled with other chromatographic techniques, such as ion-exchange or size-exclusion chromatography, to achieve even greater purity when necessary. Despite its many advantages, there are some limitations to His-tag affinity chromatography. For example, the presence of the His-tag can sometimes interfere with the protein's biological activity, particularly if the tag is located in a region critical for protein function or stability. In such cases, the His-tag can be cleaved off using proteases, and the purification process can be repeated to remove the cleaved tag.[10] Additionally, although His-tag affinity chromatography is effective in many cases, certain proteins may require optimized conditions, such as specific metal ions or buffer compositions, to ensure optimal binding and elution.

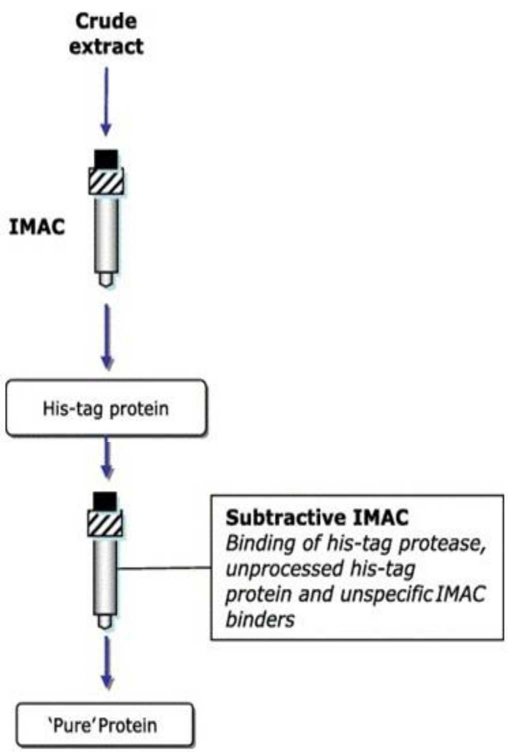

Figure 3. Outline of the steps of loading His-tagged protein on IMAC. (Adapted from Current strategies for the use of affinity tags and tag removal for the purification of recombinant proteins (p. 8), by J. Arnau, C. Lauritzen, G. E. Petersen, & J. Pedersen, 2006, Protein Expression and Purification, 48(1), 1–13 (https://doi.org/10.1016/j.pep.2005.12.002). Copyright 2006 by Elsevier.)

1.1.4. Ion Exchange Chromatography

Ion exchange chromatography is a widely used analytical and preparative technique for separating and purifying charged biomolecules, such as proteins, nucleic acids, and small ions. This method exploits the electrostatic interactions between charged molecules and a stationary phase that carries charged functional groups.[11] The principle of ion-exchange chromatography relies on the reversible binding of ions from a sample to a charged resin, typically made from materials like polystyrene or cellulose, functionalized with either positively charged (anion-exchange) or negatively charged (cation-exchange) groups.[11]

In cation-exchange chromatography, the resin is functionalized with negatively charged groups, such as sulfonate or carboxylate.[11] When a sample containing positively charged ions (cations) is introduced into the column, the cations bind to the negatively charged sites on the resin. The strength of this binding depends on the charge and size of the ions. Smaller or more highly charged cations will bind more strongly to the resin, while larger or less charged cations will bind more weakly.[12] As the sample moves through the column, different components will bind to the resin to varying degrees based on their charge and size.

To separate the bound components, the ionic strength or pH of the mobile phase is gradually adjusted.[11] This causes the cations bound to the column to compete with the mobile phase ions for binding sites on the resin, eventually displacing the bound components. The different cations will elute from the column at different times, allowing for effective separation and purification based on their affinity for the stationary phase.

Ion-exchange chromatography can be performed in either batch or column mode, with column chromatography being the most common approach for high-resolution separations.[12] The technique is highly versatile, with a range of elution strategies that can be optimized for specific applications. One of the most significant advantages of ion-exchange chromatography is its ability to purify proteins with high specificity and resolution. By carefully controlling the buffer composition, pH, and ionic strength, this technique allows researchers to isolate proteins based on their unique net charge properties.[12] Moreover, ion-exchange chromatography plays a crucial role in the purification of nucleic acids, polysaccharides, and even small organic ions, making it a versatile tool in both basic research and industrial applications. It is particularly useful in applications requiring high-resolution separation of biomolecules, such as protein purification, enzyme characterization, and the isolation of charged metabolites.[11]

1.1.5. Size Exclusion Chromatography

Size exclusion chromatography (SEC), also known as gel filtration chromatography, is an analytical technique designed for the separation and characterization of biomolecules and polymers based on their size or molecular weight. This method is valuable in applications where the primary goal is to isolate and purify macromolecules, such as proteins, nucleic acids, and synthetic polymers, without altering their structure or activity. SEC operates on the principle of molecular sieving, where molecules are separated as they pass through a porous stationary phase composed of beads with defined pore sizes.[13] Molecules are separated based on their ability to enter the pores of the stationary phase, with larger molecules eluting first and smaller molecules taking longer to pass through the column.

In size exclusion chromatography, the stationary phase typically consists of a gel or polymeric material, such as cross-linked dextran, agarose, or polyacrylamide.[13] These materials are chosen for their ability to form a network of pores of varying sizes that can selectively accommodate different molecules based on their dimensions.[13] As the sample mixture is loaded onto the column, the larger molecules are excluded from entering the pores, and thus, they travel a shorter path through the column and elute faster.[14] Smaller molecules, on the other hand, can penetrate the pores, causing them to have a longer path to travel and thus eluting later.[14] The result is a separation of molecules by size, with the elution profile providing information on the distribution of molecular weights within the sample.

One of the primary advantages of SEC is its ability to separate molecules in their native, unaltered state, as it does not rely on interactions between the molecules and the stationary phase, such as ion-exchange or affinity chromatography. This makes SEC ideal for purifying delicate proteins, nucleic acids, and other biomolecules that may be sensitive to changes in their environment. Furthermore, SEC is a non-destructive technique, meaning that molecules are not chemically modified or degraded during the separation process, making it particularly useful in applications requiring high-quality, functional material.[14]

1.1.6. SDS-PAGE

Sodium dodecyl sulfate-polyacrylamide gel electrophoresis (SDS-PAGE) is used for the separation and characterization of proteins. This method allows for the assessment of protein purity, molecular weight determination, and detection of contaminants, making it an essential tool in protein research and purification workflows. The fundamental principle behind SDS-PAGE is the ability of the detergent sodium dodecyl sulfate (SDS) to denature proteins by disrupting their tertiary and quaternary structures. SDS binds to proteins, imparting a uniform negative charge proportional to the protein's length, allowing proteins to be separated based on only their size during electrophoresis.[15] SDS-PAGE operates on the basic principle of electrophoresis, which involves the movement of charged molecules through a gel matrix under the influence of an electric field.[15] The denatured proteins will travel towards the positive electrode.

SDS is an anionic detergent that binds to hydrophobic regions of proteins and unfolds them into linear chains.[15] This process ensures that the proteins acquire a uniform negative charge, masking the intrinsic charge that could otherwise affect migration. The amount of SDS bound to each protein is roughly proportional to its molecular weight, and this results in proteins migrating through the polyacrylamide gel based primarily on their size, with larger proteins moving more slowly and smaller ones traveling faster.[16] The gel used in SDS-PAGE is made of polyacrylamide, a cross-linked polymer that forms a mesh-like structure.[15] The size of the pores in the polyacrylamide gel determines the resolution of the separation; smaller proteins can pass through smaller pores more easily, while larger proteins experience greater resistance and move more slowly. The result is a separation of proteins according to their molecular weight. After electrophoresis, proteins are typically visualized using staining techniques such as Coomassie Brilliant Blue or silver staining, which allow for the detection of protein bands.[15]

SDS-PAGE is an indispensable tool in the analysis and characterization of proteins. One of its most common uses is for determining the molecular weight of proteins. By comparing the migration distance of a protein of interest with that of a set of molecular weight markers (protein standards), an estimate of the protein's molecular weight can be made.[16] This is critical in protein identification and characterization, as it helps confirm the identity and purity of recombinant proteins or proteins obtained from complex mixtures. In addition, SDS-PAGE is also widely used in protein purity analysis. The technique can separate proteins based on size and allows for the visualization of contaminant proteins or degradation products. This is particularly important in the production of therapeutic proteins or in protein-based diagnostics, where high purity is essential.[16]

1.2 Crystallization

Protein crystallization is an important technique in structural biology that has significantly advanced our understanding of protein structures and functions. Proteins are essential biomolecules involved in nearly every cellular process, including enzymatic reactions, signal transduction, and structural support. To fully understand their mechanisms, it is crucial to determine their three-dimensional structures at atomic resolution. Protein crystallization helps by preparing proteins for X-ray crystallography, a powerful method used to visualize their atomic arrangements.[17] The ability to form high-quality protein crystals is fundamental for providing insights into the atomic-level structure and function of proteins, which is vital for drug design, understanding disease mechanisms, and advancing biotechnology.[17]

Protein crystallization involves arranging protein molecules into a well-ordered, repeating lattice to form crystals suitable for structural analysis.[18] This occurs when the protein is in a supersaturated solution, meaning the concentration of the protein exceeds its solubility.[11] These crystals are then used in X-ray diffraction studies to determine atomic-level details. The process requires highly purified proteins and carefully controlled conditions, such as specific pH levels, temperatures, and the addition of precipitants like salts or organic solvents.[19] Protein crystallization consists of two critical steps: nucleation and crystal growth. Nucleation involves the initial formation of small, stable clusters of protein molecules, which is often the most challenging phase due to the precise conditions required.[20] Following nucleation, the crystal grows as additional protein molecules join the cluster in an orderly manner, forming a macroscopic crystal.[20] Optimizing factors such as ionic strength, buffer composition, precipitating agent, pH, and temperature is essential for successful crystallization.[19]

One of the most widely used methods for crystallizing proteins is the hanging drop method. This method allows for the gradual formation of protein crystals under controlled conditions, facilitating their growth in a reproducible and consistent manner. Protein crystallization is induced by manipulating the concentration of the protein and the conditions of the solution. This technique is particularly common because it allows for fine-tuning of the experimental conditions, such as the concentration of salt, pH, and other precipitating agents that influence crystal formation.[19]

The hanging drop method involves mixing a small drop of protein solution with an equal or smaller volume of precipitant solution on a glass cover slide and suspending it over a reservoir of precipitant solution. The concentration of protein and precipitant in the mixed drop is initially lower than in the well solution. Therefore, the drop will try to reach vapor equilibrium with the liquid reservoir of precipitant. This causes the water to evaporate from the drop and increase the concentration of both components until equilibrium with the well solution is achieved. This process occurs slowly and gradually, favoring crystallization over precipitation. The idea behind the hanging drop method is that the drop of protein solution gradually equilibrates with the surrounding environment in the reservoir, allowing for the gradual diffusion of precipitant into the drop.[21] This slow diffusion process leads to an increase in protein concentration within the drop, ultimately reaching supersaturation, which triggers crystallization.[21]

The advantage of the hanging drop method is the precise control it offers over the crystallization process. The concentration of the precipitant in the drop increases gradually, allowing for more refined conditions that promote crystal growth.[19] Additionally, the method allows for observation of the crystallization process in real-time, providing insight into the optimal conditions required for crystallization.

The significance of protein crystallization extends beyond structural determination because it also plays an important role in various scientific and medical applications. The structural information obtained through protein crystallization can guide the development of drugs, help in the design of enzymes for industrial applications, and inform the design of molecular diagnostics. The ability to determine a protein's 3D structure with precision allows scientists to understand how a protein binds to its ligands, how it catalyzes reactions, and how mutations might affect its function.[22] This level of understanding can lead to the development of specific, potent, and selective inhibitors or activators of protein function, which is central to drug design. Additionally, these insights provide a deeper understanding of disease mechanisms at the molecular level, facilitating the development of targeted therapies.[23] Protein crystallization also supports advancements in biotechnology, such as the engineering of enzymes for industrial applications or the enhancement of agricultural products.[23] By uncovering the details of protein structures, crystallography continues to drive progress in science, medicine, and technology, solidifying its position as an indispensable tool in modern research.

1.3 Nsp13

1.3.1 COVID-19

The outbreak of the coronavirus disease (COVID-19) in late 2019, caused by the severe acute respiratory syndrome coronavirus 2 (SARS-CoV-2), has led to a global pandemic with far-reaching consequences.[24] COVID-19 has resulted in millions of infections and deaths worldwide, overwhelming healthcare systems, and causing significant social, economic, and psychological impacts. The pandemic has brought many challenges in terms of public health, with governments and institutions trying to find ways to stop the spread, develop treatments, and distribute vaccines. COVID-19 primarily spreads through respiratory droplets when an infected person coughs, sneezes, or talks.[24] It affects the respiratory system, with symptoms ranging from mild coughs to severe pneumonia and acute respiratory distress syndrome (ARDS).[25] It can also lead to multi-organ failure and death, especially in vulnerable populations such as the elderly and those with underlying medical conditions.[25]

1.3.2 Coronaviruses

The cause of COVID-19 is the SARS-CoV-2 virus, a member of the coronavirus family. Coronaviruses are large, enveloped viruses characterized by their spike-shaped glycoproteins that protrude from their lipid bilayer, giving the virus its name (corona, meaning crown in Latin).[26] The viral genome is single-stranded RNA, which encodes for several proteins necessary for viral replication and pathogenesis.[26] There are two major classes of proteins in coronaviruses: structural and nonstructural. The structural proteins, including the spike (S) protein, membrane (M) protein, and nucleocapsid (N) protein, are responsible for the virus's structure and ability to infect host cells.[28] The nonstructural proteins (nsps) play important roles in viral replication and the suppression of the host immune response.[28]

The spike (S) protein of SARS-CoV-2 is important because it binds to the angiotensin-converting enzyme 2 (ACE2) receptor on human cells, facilitating the virus's entry.[27] Following entry, the virus uncoats its RNA genome, which is then translated and replicated within the host cell.[27] Coronaviruses, like SARS-CoV-2, use a replication complex composed of several nonstructural proteins to replicate their RNA genome and produce the components needed for new viral particles.[28] These proteins include polymerases, helicases, and other enzymes that interact with the host cell machinery.

1.3.3 Nsp13

One of the key nonstructural proteins that contributes to the viral replication of coronaviruses is nonstructural protein 13 (nsp13). It is an RNA helicase that plays a vital role in the replication and transcription of the viral genome. The importance of nsp13 is that it unwinds the viral RNA, a critical step in the replication process.[29] Nsp13 is highly conserved across different coronaviruses, and its functional importance in viral replication makes it an attractive target for therapeutic interventions.[29]

Structurally, nsp13 belongs to the Superfamily 1 helicase family, and it contains several conserved domains necessary for its helicase activity. The protein is composed of several subdomains that contribute to its RNA-binding and unwinding properties.[30] The helicase activity of nsp13 is essential for the viral life cycle because it resolves secondary RNA structures that might otherwise impede replication.[30] By unwinding the RNA genome, nsp13 allows the viral RNA polymerase to access the RNA template, thereby enabling viral replication and the production of viral mRNA.[31] Nsp13 also plays a role in the synthesis of viral RNA intermediates, making it integral to both the replication and transcription of the virus.[31]

In the context of SARS-CoV-2, nsp13 works alongside other nonstructural proteins, including the RNA-dependent RNA polymerase (RdRp) and other cofactors, to form the replication-transcription complex (RTC).[31] This complex is responsible for the synthesis of new viral RNA and the production of proteins that form new viral particles. The helicase activity of nsp13 is essential for maintaining the efficiency of the replication process. Without this activity, the virus would be unable to efficiently replicate its genome, leading to decreased viral production and an inability to propagate within the host.

Nsp13 is also involved in various processes that affect viral pathogenesis. Studies have shown that nsp13 interacts with the host cell's machinery to regulate cellular processes and evade the immune system.[32] For example, nsp13 has been implicated in the inhibition of host cell RNA sensing mechanisms, which would normally trigger an antiviral immune response.[32] By regulating these host pathways, nsp13 helps the virus evade detection by the host immune system, allowing it to replicate unchecked and cause disease.

The study of nonstructural protein 13 is critical in the development of antiviral therapies aimed at combating COVID-19. Given its essential role in the replication of the virus, nsp13 is a promising target for therapeutic intervention.[29] Inhibiting nsp13 could potentially halt viral replication, thus limiting the spread of the virus within the host and reducing the severity of disease. Several small molecules and peptides have been identified as potential inhibitors of nsp13, showing promise in preclinical studies.[33] These compounds could form the basis for novel antiviral drugs, providing a necessary tool in the fight against COVID-19.

1.4. Purpose of the Study

The primary objective of this study was to replicate the previously established methods for the expression and purification of nsp13 protein.[29] This study aimed to refine these protocols to achieve higher yields and purity of the protein, ensuring its suitability for subsequent structural analysis. The secondary goal was to optimize the conditions for protein crystallization, with the aim of obtaining high-quality crystals that would facilitate X-ray crystallography studies. By improving crystallization conditions, this study sought to enhance the resolution of the nsp13 structure, providing deeper insights into its functional mechanisms and its potential as a therapeutic target in the fight against COVID-19.

2 EXPERIMENTAL DETAILS

2.1 Transformation

2.1.1 Plasmid Information

In this study, the plasmid encoding SARS-CoV-2 nsp13 was obtained from Addgene (Plasmid #159614). This plasmid was originally deposited by Dr. Opher Gileadi. For additional information, see https://www.addgene.org/159614/. The plasmid includes an N-terminal His6-Zb-TEV tag and a T7 promoter for protein expression in *Escherichia coli* (Figure 4A) and the coding sequence for nsp13 (Figure 4B).

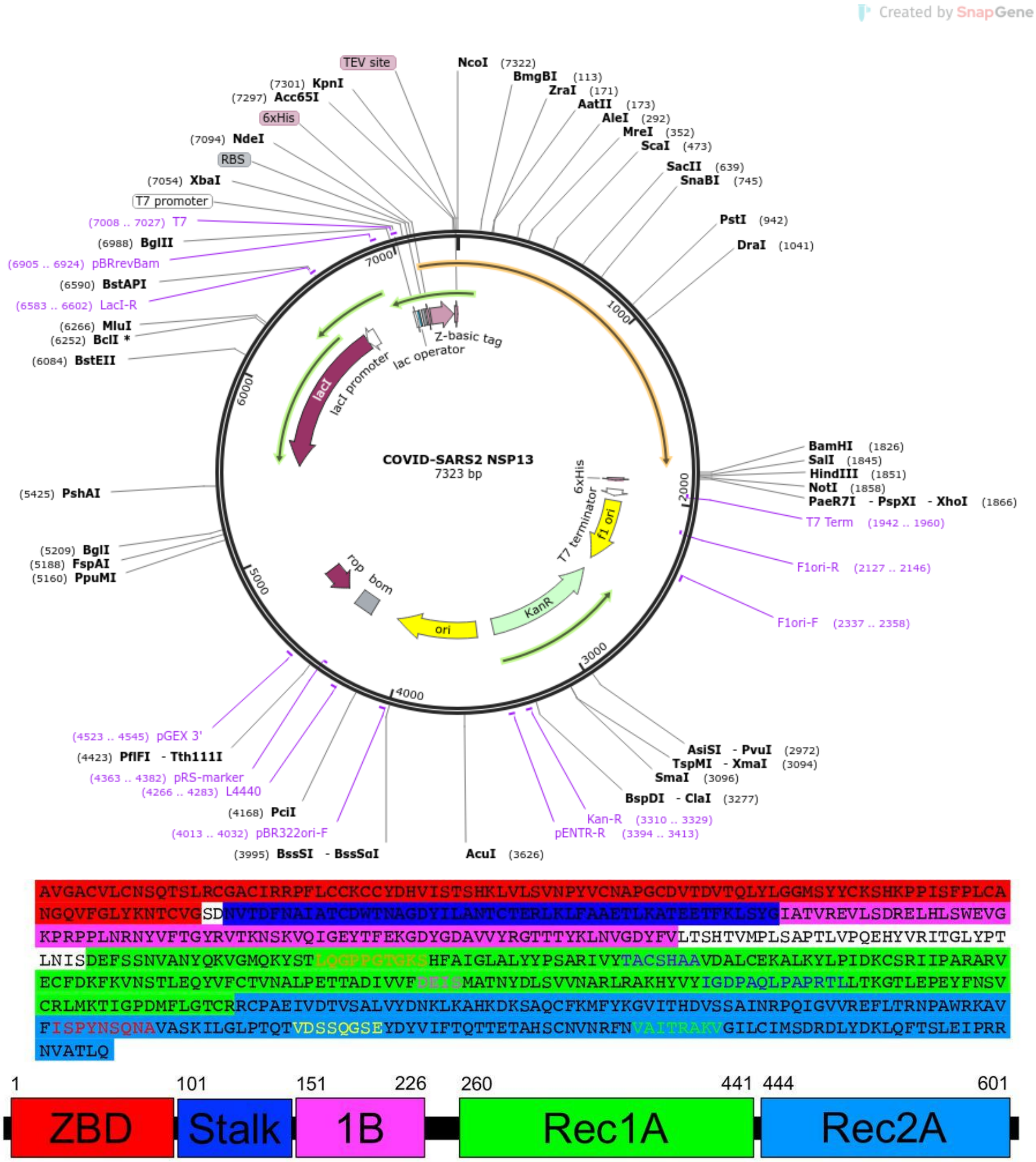

A

B

Figure 4. Map of the SARS-CoV-2 Nsp13 expression plasmid (Addgene Plasmid #159614).

2.1.2 Extraction of Plasmid

The QIAprep Spin Miniprep Kit was used to extract SARS-CoV-2 nsp13 expression plasmid from Top10 *E. coli* cells. A 1 mL aliquot of bacterial culture was transferred to a microcentrifuge tube. The cells were pelleted by centrifugation at 13,000 rpm for 3 minutes at room temperature. The supernatant was discarded, and the pellet was resuspended in 250 µL of Buffer P1. Lysis was achieved by adding 250 µL of Buffer P2, which was mixed thoroughly by inverting the tube 4–6 times. To precipitate proteins, 350 µL of Buffer N3 was added and mixed immediately. Following a 10-minute centrifugation at 13,000 rpm, 800 µL of the resulting supernatant containing the plasmid DNA was carefully transferred to a QIAprep 2.0 spin column. The column was centrifuged for 1 minute, and the flow-through was discarded. The column was then washed with 0.75 mL of Buffer PE (containing ethanol) and centrifuged for 1 minute. The flow-through was discarded, and the column was further centrifuged for 1 minute to remove residual wash buffer. The spin column was air-dried on the benchtop to allow any remaining ethanol to evaporate. The QIAprep 2.0 column was transferred to a clean 1.5 mL microcentrifuge tube, and plasmid DNA was eluted by adding 50 µL of Buffer EB (10 mM TrisCl, pH 8.5) to the center of the column. After a 1-minute incubation, the column was centrifuged for 1 minute to collect the eluted DNA. The plasmid concentration was determined using a NanoDrop 2000/2000c spectrophotometer. The extracted plasmid was stored at -20°C.

2.1.3 Preparing Agar Plates

LB media containing 1.5% (w/v) agar was prepared and sterilized through autoclaving. After sterilization, the media was allowed to cool to room temperature to avoid degrading the antibiotics. Kanamycin was added to the media at the required final concentration of 50 µg/mL, and the solution was mixed thoroughly to ensure even distribution. Approximately 20 mL of the prepared media was poured into each sterile 100 mm Petri dish under aseptic conditions. The plates were left partially uncovered for 10 minutes to allow excess moisture to evaporate and the agar to solidify. Once solidified, the plates were covered with their lids, inverted to prevent condensation from dripping onto the agar surface, and sealed with Parafilm to maintain sterility. The plates were stored inverted at 4°C.

2.1.4 Transforming SARS-CoV-2 Nsp13 Expression Plasmid into Rosetta™ 2(DE3)pLysS Competent Cells

Competent cells were retrieved from -80°C and thawed on ice. The plasmid was removed from -20°C, and 5 10 ng of plasmid DNA was added to 50 µL of competent cells. The cell-DNA mixture was incubated on ice for two minutes. A heat shock was performed by placing the tube in a 42°C heat block for 30 seconds, followed by immediate incubation on ice for 2 minutes. Subsequently, 80 µL of SOC (Super Optimal Broth with Catabolite repression) medium was added to the transformation mixture, and the cells were allowed to recover by incubation at 37°C in a shaking incubator for 1 hour.

LB agar plates (pre-warmed to room temperature) were prepared and labelled. Under the Bunsen burner, 50 µL of the cell-DNA mixture was added onto the agar surface. A sterile glass spreader, disinfected with ethanol and a Bunsen burner, was used to evenly spread the transformation mixture across the plate in multiple directions to ensure uniform distribution. The plates were covered with foil and incubated overnight at 37°C.

2.2 Expression

2.2.1 Small Culture of Cells Transformed with Plasmids Containing Nsp13

A small culture was started using a 125 mL flask containing 30 mL of Terrific Broth (TB) media supplemented with 30 µL of 50 mg/mL kanamycin. A single colony from the plate with the transformed cells was picked and inoculated in to the TB media. The flask was then incubated overnight at 37°C with shaking at 200 rpm to promote cell growth.

2.2.2 Large Culture and Expression of Cells Transformed with Plasmids Containing Nsp13

Following the overnight growth of a small culture, a larger culture was prepared in a 4000 mL Erlenmeyer flask containing 1 L of TB media supplemented with 1 mL of 50 mg/mL kanamycin. A 10 mL aliquot of the small culture was inoculated into the larger flask. The culture was incubated at 37°C with shaking at 200 rpm until it reached an optical density at 600 nm of 1.1-1.3, as measured using a BioMate 3S UV-Visible Spectrophotometer.

Protein expression was induced by adding 0.3 mM IPTG to the culture. The flask was then returned to the shaker, and the incubation temperature was lowered to 18°C at a reduced speed of 180 rpm for 16 hours. After incubation, the cells were harvested by centrifugation using a JLA-8.1000 rotor at 8000 x g for 15 minutes at 4°C. The resulting cell pellet was transferred into a Ziploc bag, weighed, and stored at -80°C.

2.3 Purification of Uncleaved Nsp13

2.3.1 Resuspension

The cell pellet was retrieved from storage at -80°C. The frozen cells were broken into smaller pieces and transferred to a 250 mL beaker. Resuspension buffer was added at a ratio of 10 mL per gram of cell pellet. Given that approximately 10 g of cells were obtained from 1 L of TB culture, 100 mL of resuspension buffer (20 mM Tris pH 7.5, 500 mM NaCl, 5% glycerol, 10 mM imidazole, 0.5 mM TCEP) was added. The suspension was incubated at 4°C for 1 hour with continuous stirring using a magnetic stir bar to ensure thorough resuspension.

2.3.2 Sonication

Following resuspension, phenylmethylsulfonyl fluoride (PMSF) was added to the solution to a final concentration of 2 µM. The resuspended cell solution was then divided equally between two 50 mL beakers. Cell lysis was performed using a Branson Digital Sonifier, with sonication parameters set to 5 minutes total duration at 15% amplitude, employing a pulse cycle of 10 seconds on and 5 seconds off. The solution was cooled on ice between each sonication cycle, for a total of five cycles.

After sonication, the cell lysate was centrifuged at 25,000 x g for 1 hour at 4°C using a JA-25.50 rotor. The resulting supernatant was filtered through a 0.45 µm membrane filter to remove any remaining particulates.

2.3.3 Immobilized Metal Affinity Chromatography

The nsp13 protein was purified using the ÄKTA Start protein purification system with a 1 mL HisTrap™ HP column. The column was equilibrated with 5 column volumes (CV) of resuspension buffer (20 mM Tris pH 7.5, 500 mM NaCl, 5% glycerol, 10 mM imidazole, 0.5 mM TCEP). The clarified lysate was loaded onto the column at a flow rate of 1 mL/min.

Subsequently, the column was subjected to sequential washing steps to remove nonspecifically bound proteins:

1. Wash 1: 60 CV of resuspension buffer.

2. Wash 2: 30 CV of buffer containing 50 mM HEPES pH 7.5, 500 mM NaCl, 5% glycerol, 25 mM imidazole, and 0.5 mM TCEP.
3. Wash 3: 30 CV of buffer containing 50 mM HEPES pH 7.5, 500 mM NaCl, 5% glycerol, 50 mM imidazole, and 0.5 mM TCEP.
4. Wash 4: 10 CV of buffer containing 50 mM HEPES pH 7.5, 1 M NaCl, and 0.5 mM TCEP.
5. Wash 5: 15 CV of buffer containing 50 mM HEPES pH 7.5, 500 mM NaCl, 5% glycerol, 75 mM imidazole, and 0.5 mM TCEP.
6. Wash 6: 15 CV of buffer containing 50 mM HEPES pH 7.5, 500 mM NaCl, 5% glycerol, 125 mM imidazole, and 0.5 mM TCEP.

The protein was eluted using a buffer containing 50 mM HEPES pH 7.5, 500 mM NaCl, 5% glycerol, 250 mM imidazole, and 0.5 mM TCEP. The elution was monitored via UV absorbance, and fractions were collected into a 50 mL Falcon tube once the UV signal began to rise, indicating the presence of protein.

2.3.4 Cation Exchange Chromatography

Following affinity chromatography, the eluted ***nsp***13 protein was further purified using ion-exchange chromatography. A 1 mL HiTrap SP HP column was first equilibrated with five CV of the previous elution buffer containing 50 mM HEPES pH 7.5, 500 mM NaCl, 5% glycerol, 250 mM imidazole, and 0.5 mM TCEP. The eluted ***nsp***13 protein was then applied to the column at a flow rate of 1 mL/min. The column was washed with 15 CV of the equilibration buffer to remove any unbound contaminants. Subsequently, the protein was eluted using a buffer containing 50 mM HEPES pH 7.5, 1 M NaCl, and 0.5 mM TCEP, facilitating the separation of nsp13 based on its charge.

2.3.5 Buffer Exchange

Buffer exchange was performed using a 30 kDa Amicon Ultra Centrifugal Unit. Initially, 15 mL of buffer containing 50 mM Tris pH 7.5, 500 mM NaCl, and 0.5 mM TCEP was added to the filter device and centrifuged at 3,500 x g for 10 minutes at 4°C using a swinging bucket rotor. Following centrifugation, the filtrate was discarded, and the uncleaved ***nsp***13, purified using a HiTrap SP HP column, was loaded into the filter device. The device was then filled to capacity with the same buffer (50 mM Tris pH 7.5, 500 mM NaCl, 0.5 mM TCEP) and centrifuged again under the same conditions. This buffer exchange process was repeated multiple times using buffer without imidazole until the imidazole concentration was reduced to near zero. In addition, the sample was concentrated to 0.5 mg/mL. Finally, the sample containing uncleaved nsp13 was collected from the filter device.

2.3.6 Determining Protein Concentration

Protein concentration was quantified using the Bradford assay with a BioMate 3S UV-Visible Spectrophotometer. A cuvette containing 500 µL of Bradford reagent served as the blank. In a separate cuvette, 16 µL of the protein sample was mixed with 500 µL of Bradford reagent. The absorbance at 595.0 nm was measured to determine protein concentration.

2.4 Cleavage with TEV Protease

TEV protease (2 mg/mL) was used at a ratio of 1 mg of TEV per 10 mg of protein. Following the addition and thorough mixing of TEV protease, the sample was incubated at 4°C for 16 hours.

2.5 Purification of Cleaved Nsp13

2.5.1 Removing TEV protease and His-tags from cleaved nsp13 with Immobilized Metal Affinity Chromatography

A HisTrap™ HP 1 mL column was equilibrated with five CV of buffer containing 50 mM HEPES pH 7.5, 500 mM NaCl, and 0.5 mM TCEP. The nsp13 sample with TEV protease was loaded onto the column at a flow rate of 1 mL/min. The flowthrough was collected, followed by a 10 CV wash with equilibration buffer, which was also collected. To elute any remaining bound proteins, the column was subsequently washed with a buffer containing 50 mM HEPES pH 7.5, 500 mM NaCl, 500 mM imidazole, and 0.5 mM TCEP.

2.5.2 Size-Exclusion Chromatography

The cleaved **nsp**13 protein was further purified using the ÄKTA Prime Plus protein purification system equipped with a HiLoad™ 16/600 Superdex™ 75 pg column. The column was equilibrated with a buffer containing 50 HEPES pH 7.5, 500 mM NaCl, and 0.5 mM TCEP before sample injection. The column pressure limit was set to 0.30 MPa, and the flow rate was maintained at 0.5 mL/min. Fractions were collected every 2 mL. A total of approximately 2 mL of the protein sample was loaded onto the column, with an injection volume set at 4.0 mL. The total elution volume was 130 mL. Fractions corresponding to UV absorbance peaks were collected for further analysis.

2.6 SDS-PAGE

2.6.1 Sample Preparation

SDS-PAGE samples were prepared by aliquoting 60 µL of the sample into a new Eppendorf tube, followed by the addition of 12 µL of 5x cracking dye. For solid samples, 1 mL of PBS was used to resuspend the material, and 48 µL of the resulting suspension was mixed with 12 µL of 5x cracking dye. The prepared samples were then heated at 100°C for 10 minutes in a heat block to ensure complete denaturation.

2.6.2 Running SDS-PAGE

SDS-PAGE was performed using a SurePAGE™ Bis-Tris 10x8 gel with 4–20% polyacrylamide. The gel, along with an empty glass plate, was secured within a vertical gel cassette assembly and positioned in the vertical gel chamber. The inner compartment of the gel cassette and the surrounding assembly were filled with Tris-MOPS-SDS running buffer. After carefully removing the comb, 3 µL of PageRuler™ Prestained Protein Ladder was loaded into the designated lane. A 20 µL aliquot of each sample was then loaded into individual wells. The lid of the gel chamber was securely placed with the power cables connected to the corresponding terminals on the power supply. Electrophoresis was conducted at 200 V for 35 minutes.

2.6.3 Protein Staining and Destaining

After disassembling the SDS-PAGE set up, the gel was removed from between the two plastic plates, and the gel was transferred to a small, plastic tray. The gel was fully submerged in Coomassie Brilliant Blue staining solution, ensuring complete coverage. The tray was microwaved for 15 seconds until the solution reached boiling, allowing efficient penetration of the dye into the protein bands. To remove excess stain, the Coomassie solution was discarded, and 10% acetic acid was added to the tray. The gel was microwaved again for 20 seconds until boiling to initiate the destaining process. The tray was covered and placed on a shaker overnight to enhance the removal of background staining. Paper towels were placed inside the tray to help absorb excess dye. The gel was then examined under appropriate lighting for protein band visualization.

2.7 Crystallization

2.7.1 Preparing the Protein Sample

The uncleaved nsp13 protein was collected from the S75 column. After purity was checked by SDS-PAGE, the sample was transferred to a 30 kDa Amicon Ultra Centrifugal Unit and concentrated at 3,500 x g in 4°C. Concentration continued until the final protein concentration reached approximately 10 mg/mL.

2.7.2 Setting up the Crystal Tray

A 500 µL aliquot of the reservoir solution was pipetted into each well of the crystallization tray. The reservoir solution consisted of 0.03 M sodium nitrate, 0.03 M sodium phosphate dibasic, 0.03 M ammonium sulfate, 0.05 M sodium HEPES, 0.05 M MOPS (pH 7.5), and 16% ethylene glycol. Varying concentrations of polyethylene glycol (PEG) 8000 or 10K was used.

Six wells had 8% PEG 8000, six wells had 12% PEG 8000, and six wells had 15% PEG 8000. A 1 μL aliquot of the protein solution was then mixed with 1 μL of the reservoir solution on a 22 mm siliconized glass circle cover slide, which was then inverted and sealed over the well to create a hanging drop without direct contact with the reservoir solution. The tray was incubated at 20^{o}C in a controlled environment, and crystallization progress was monitored weekly using a light microscope.

3 RESULTS AND DISCUSSION

3.1 Protein Expression

The SARS-CoV-2 nsp13 was successfully expressed into *E. coli* Rosetta^{TM} 2(DE3)pLysS cells following induction with IPTG. Expression was confirmed by SDS-PAGE analysis (Figure 5), where a clear band at approximately 76 kDA was observed, corresponding to the predicted molecular weight of nsp13 with the His6-Zb-TEV tag. Lane b represents a pre-induction control sample collected from the culture at an $OD_{600.0\ nm}$ of approximately 1.2, while lane c corresponds to the post-induction sample collected after incubation with 0.3 mM IPTG for 16 hours at 18°C with shaking at 180 rpm. The increased intensity of the 76 kDa band in lane c compared to lane b confirms successful induction and overexpression of nsp13.

Even though the expected molecular weight of nsp13 is approximately 76 kDa, there is an observed deviation since the distinct band is positioned between 55–70 kDa on the SDS-PAGE. This can be attributed to several factors. One possible explanation is irregular electrophoretic migration, where proteins do not always migrate according to their theoretical molecular weights due to variations in SDS binding, charge distribution, or intrinsic structural properties.[15] Another contributing factor may be the composition of the gel matrix, as variations in acrylamide concentration can influence protein mobility and lead to shifts in apparent molecular weight.[15] Furthermore, protein truncation or degradation could result in lower molecular weight fragments being detected on the gel.[15] Similar observations have been reported for other viral helicases, where compact folding or post-translational modifications lead to altered migration patterns.[16]

Also, the SDS-PAGE results revealed faint bands in some lanes, which warrant further discussion. A contributing factor could be the staining and imaging conditions of the gel. If the gel was not stained for a sufficient amount of time or if destaining was overly aggressive, this could result in bands appearing fainter than expected. Coomassie Brilliant Blue requires optimal staining and destaining conditions to visualize proteins effectively. If a low-sensitivity stain or insufficient staining time was used, this could explain the weak band intensity observed.[16]

Despite the observed deviation, SDS-PAGE analysis is still a widely used technique for assessing recombinant protein expression, as it separates proteins based on molecular weight. The presence of a distinct band at the expected size of 76 kDa following IPTG induction indicates successful expression of nsp13. The increased intensity of this band in lane c compared to lane b suggests that the protein was produced in greater quantities following induction. In contrast, the control lane (lane b) shows a much fainter band at this molecular weight which indicates minimal basal expression before induction and demonstrates that significant expression occurs only upon IPTG induction. These results demonstrate that *E. coli* Rosetta™ 2(DE3)pLysS cells serve as an effective expression system for producing recombinant nsp13 under the given conditions.

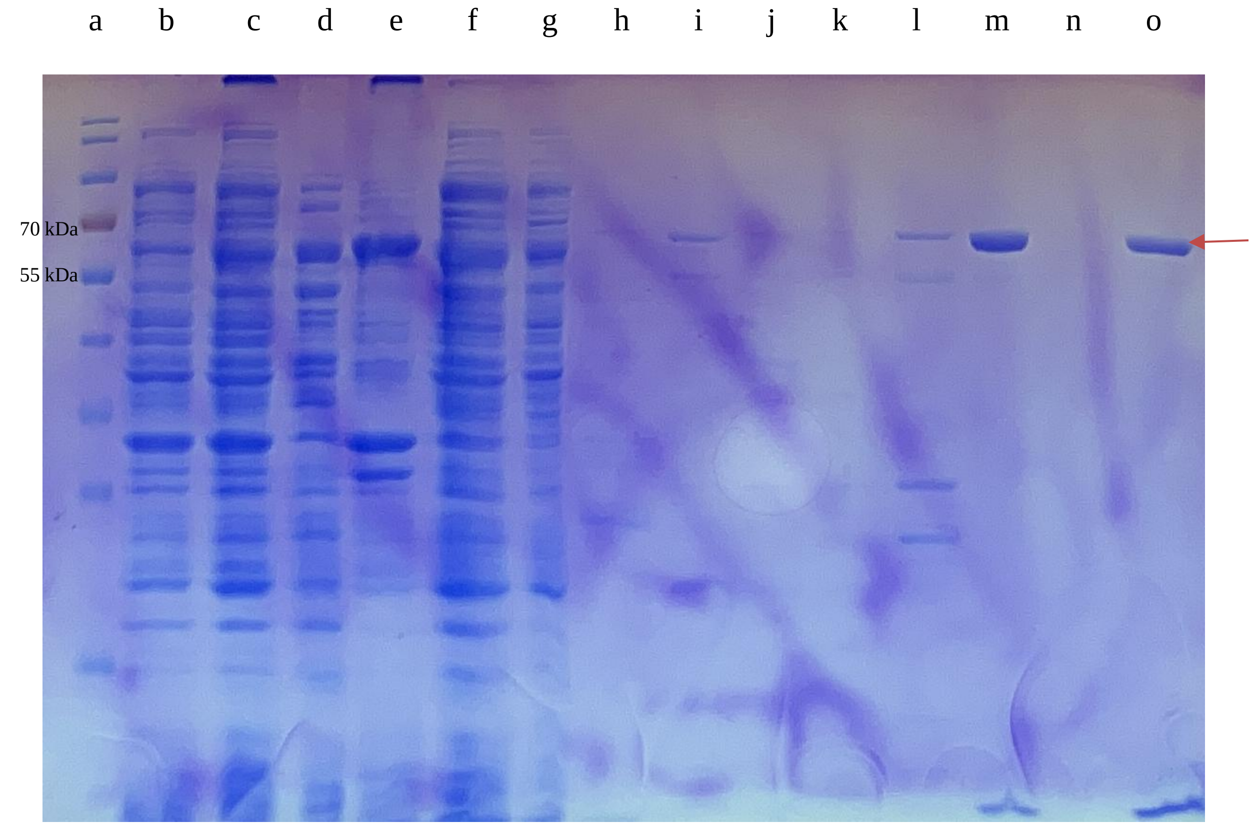

Figure 5. SDS-PAGE gel showing the expression and purification of uncleaved nsp13 following the first affinity chromatography and ion-exchange chromatography. Lane **a:** PageRuler Prestained Protein Ladder. Lane **b:** pre-induction control. Lane **c**: post-induction sample. Lane **d**: soluble fraction. Lane **e**: insoluble fraction. Lane **f**: flowthrough of HisTrap. Lane **g**: wash with 10 mM imidazole. Lane **h**: wash with 25 mM imidazole. Lane **i**: wash with 50 mM imidazole. Lane **j**: wash with 1 M NaCl. Lane **k**: wash with 50 mM imidazole. Lane **l**: wash with 125 mM imidazole. Lane **m**: elution with 250 mM imidazole. Lane **n**: SP flowthrough: Lane **o**: SP elution with 1 M NaCl. Red arrow points to nsp13.

3.2 Protein Purification

The purification of uncleaved nsp13 was successfully performed through a series of chromatography steps. First, following cell lysis via sonication, the clarified lysate was purified with IMAC using a HisTrap™ HP column. The elution profile shows a distinct UV absorbance peak corresponding to nsp13 elution in the presence of 250 mM imidazole (Figure 6). The eluted nsp13 was relatively pure as demonstrated in lane m of the SDS-PAGE (Figure 5). There are relatively few bands that would represent impurities and one strong distinct band at approximately 76 kDa that represents nsp13, demonstrating successful binding and purification from the cell lysate. Sequential washing steps with increasing imidazole concentrations effectively removed nonspecifically bound proteins, as shown by the SDS-PAGE analysis that shows multiple bands in the wash steps in lanes g, h, i, j, k, and l (Figure 5).

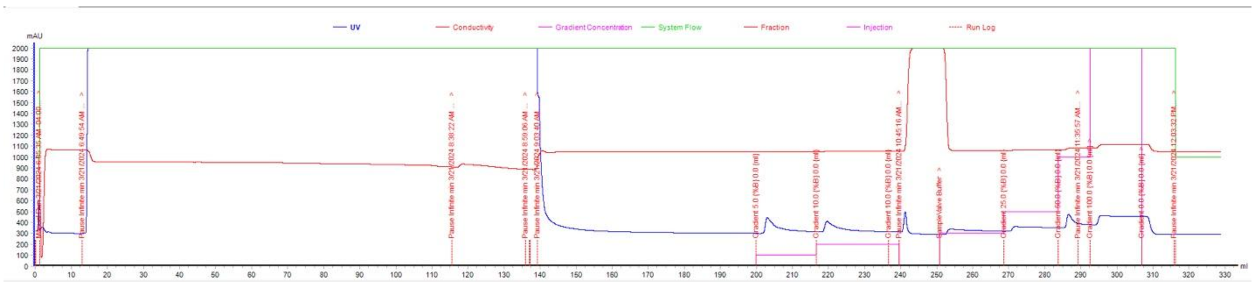

Figure 6. Elution profile of uncleaved nsp13 from HisTrap^{TM} HP 1 mL column. The protein was loaded from 12.5 mL to 140 mL. The column was washed from 140 mL to 200 mL with 10 mM imidazole. The column was washed from 200 to 217.5 mL with 25 mM imidazole. The column was washed from 217.5 mL to 240 mL with 50 mM imidazole. The column was washed from 240 mL to 250 mL with 1 M NaCl. The column was washed from 250 mL to 270 mL with 75 mM imidazole. The column was washed from 270 mL to 283 mL with 125 mM imidazole. The protein was eluted from 283 mL to 292.5 mL with 250 mM imidazole. The column was washed from 292.5 mL to 307.5 mL with 500 mM imidazole.

To enhance purity, the eluted nsp13 underwent cation exchange chromatography using a HiTrap SP HP column. The Zb tag on nsp13 facilitates efficient purification of the target protein because it gives the protein a positive charge, which allows the target protein to bind to the negative resins on the column. The protein bound efficiently to the column and was subsequently eluted with a high-salt buffer (1 M NaCl), facilitating further removal of contaminants (Figure 7). SDS-PAGE analysis confirmed purification of the target protein with minimal impurities in lane o since there is one distinct band for nsp13 (Figure 5). Following ion exchange, buffer exchange was performed using an Amicon Ultra Centrifugal Unit to remove imidazole, ensuring the imidazole would not interfere with the subsequent cleavage step.

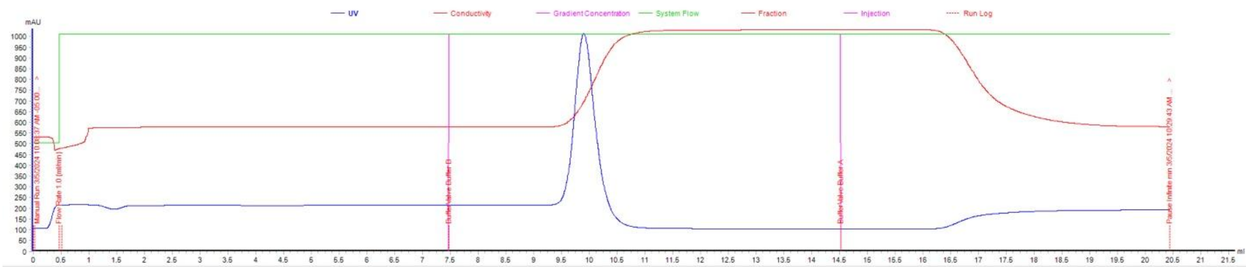

Figure 7. Elution profile of uncleaved nsp13 from HiTrap™ SP 1 mL column. The column was washed from 0.5 mL to 7.5 mL with 50 mM HEPES pH 7.5, 500 mM NaCl, 5% glycerol, 250 mM imidazole, and 0.5 mM TCEP. The protein was eluted from 7.5 mL to 14.5 mL with 50 mM HEPES pH 7.5, 1 M NaCl, and 0.5 mM TCEP.

Following TEV protease cleavage, cleaved nsp13, uncleaved nsp13, and TEV protease were separated by performing a secondary IMAC step (Figure 8). The cleaved nsp13 appeared in the flowthrough, while remaining His-tagged proteins and TEV protease remained bound to the column (Figure 9). The cleaved nsp13 is expected to have molecular weight of 67 kDa. The SDS-PAGE analysis shows that the cleavage reaction was 90% successful because in lane d, there is a small band for the uncleaved nsp13 and a much bigger band underneath it, representing the cleaved nsp13 (Figure 9). In addition, in lane e and in lane f, a majority of the sample collected from the IMAC step consists of cleaved nsp13 since it is the largest band despite there being some impurities in the sample (Figure 9). The flowthrough fraction and wash fraction containing nsp13 were further purified using size-exclusion chromatography (SEC) with a Superdex™ 75 pg column. The chromatogram exhibited a distinct peak at the expected elution volume, corresponding to nsp13 (Figure 10). SDS-PAGE confirmed a highly purified product with no contaminants in lanes d, e, f, and g from fractions collected from S75 (Figure 11). When purifying 6 L of TB media, the amount of uncleaved nsp13 collected before the addition of TEV protease was 6 mg. The yield of cleaved nsp13 after performing SEC was roughly 0.5 mg.Thus, the ratio of cleaved to uncleaved nsp13 of 0.5 to 6 indicates that 91.67% of the protein was lost after TEV cleavage.

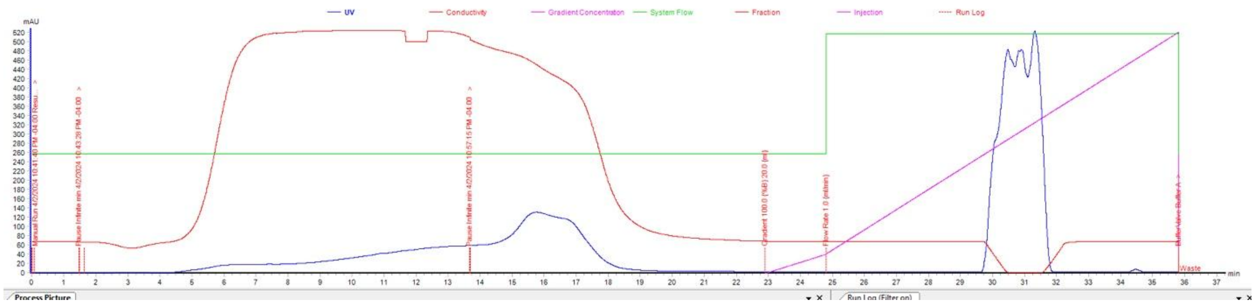

Figure 8. Elution profile of cleaved nsp13 from HisTrap™ HP 1 mL column. The protein was loaded from 1.5 mL to 14 mL. The column was washed from 14 mL to 23 mL with 50 mM HEPES pH 7.5, 500 mM NaCl, and 0.5 mM TCEP. The His-tagged proteins eluted with 500 mM from 29.5 mL to 32 mL.

a b c d e f

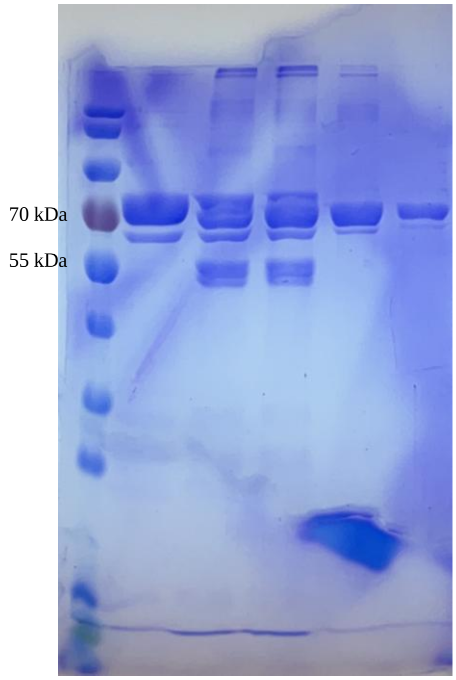

Figure 9. SDS-PAGE gel showing the cleavage of nsp13. Lane **a:** Prestained Protein Ladder. Lane **b:** uncleaved nsp13 before addition of TEV. Lane **c**: cleavage with TEV at 6 hours. Lane **d**: cleavage with TEV at 16 hours Lane **e**: flowthrough of HisTrap. Lane **f**: wash with 50 mM HEPES pH 7.5, 500 mM NaCl, and 0.5 mM TCEP.

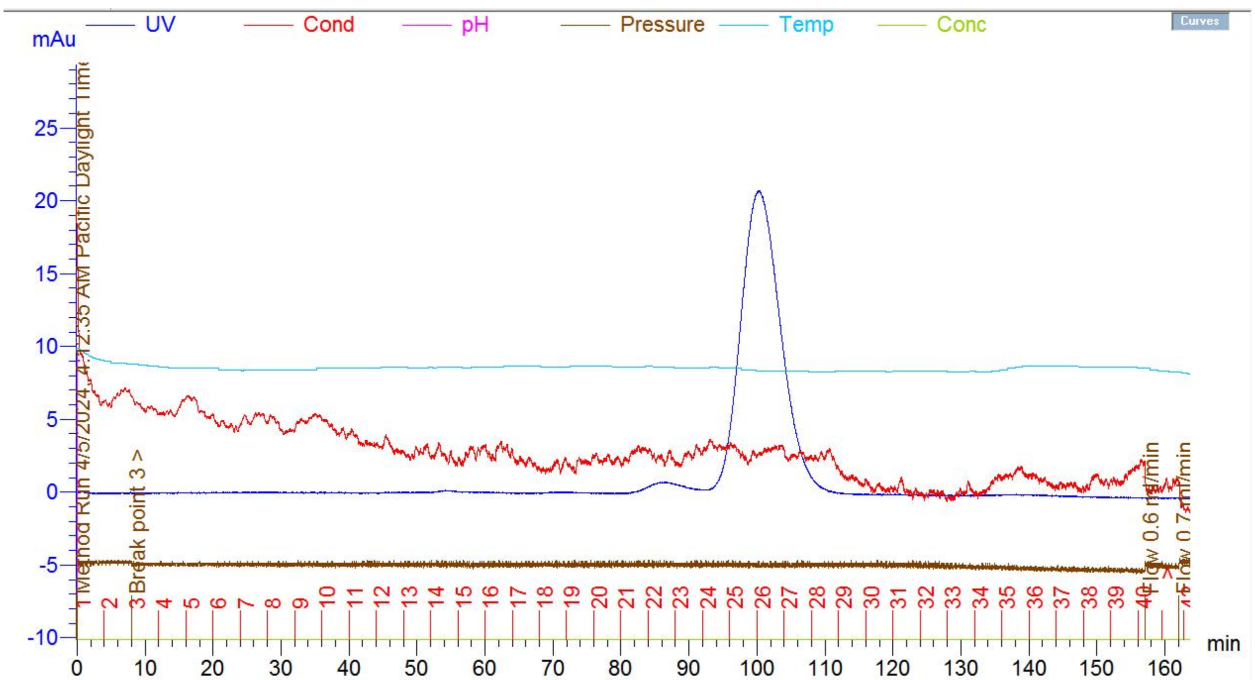

Figure 10. Elution profile of cleaved nsp13 from a HiLoad™ 16/600 Superdex™ 75 pg column. The protein eluted from fraction 24-28.

a b c d e f g

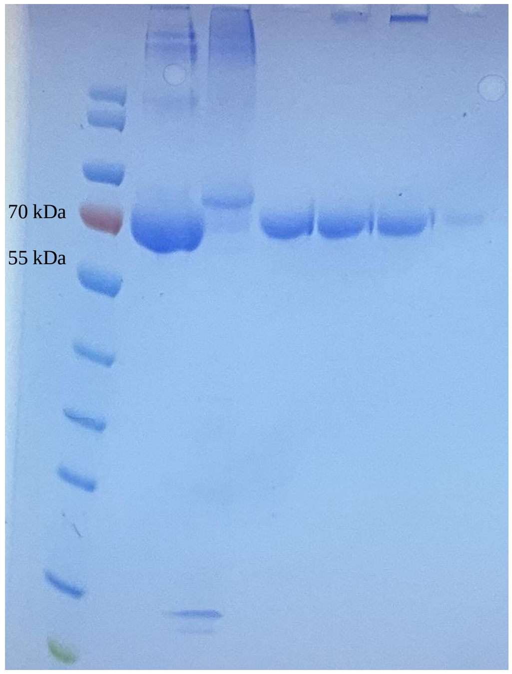

Figure 11. SDS-PAGE showing the fractions collected from size exclusion chromatography. Lane **a:** Prestained Protein Ladder. Lane **b:** cleaved nsp13 collected from HisTrap. Lane **c**: cleavage with TEV. Lane **d**: fraction 24. Lane **e**: fraction 25. Lane **f**: fraction 26. Lane **g**: fraction 27.

The purification of nsp13 was successfully achieved through a series of chromatographic techniques with each step contributing to increased purity. The initial IMAC step efficiently isolated His-tagged nsp13 from a majority of the impurities as evidenced by the SDS-PAGE analysis that shows a strong distinct band for nsp13 with few impurities (Figure 5). Cation exchange chromatography provided an additional purification step, effectively removing residual contaminants by taking advantage if nsp13's positive charge properties. The high-salt elution step successfully released bound nsp13, as confirmed by SDS-PAGE analysis (Figure 5). Also, SEC helped to remove any remaining impurities after cleavage, including any uncleaved nsp13. The result was a pure cleaved nsp13 that was ready for crystallization.

However, despite the success in purification, the overall protein yield was notably low. Several factors could have contributed to this outcome, including losses during purification steps, protein stability issues, and inefficiencies in cleavage and recovery.

One potential reason for the low yield is the inherent loss of protein during each purification step. The use of IMAC with a HisTrap™ HP column was effective in isolating nsp13 from the clarified lysate, as indicated by the distinct UV absorbance peak at 250 mM imidazole and the corresponding strong band at approximately 76 kDa on SDS-PAGE. However, the sequential wash steps, which effectively removed non-specifically bound proteins, may have also led to some loss of target protein. Even though the eluted fraction appeared relatively pure, minor contaminants observed in the SDS-PAGE gel suggest that some impurities co-eluted with nsp13, which could have contributed to lower effective yields.[9] In addition, the column has a maximum binding capacity, so there may have been too much nsp13 protein in the sample that could not bind to the column and was lost as a result.

Cation exchange chromatography further improved the purity of nsp13, as seen in SDS-PAGE analysis. However, binding efficiency can be influenced by factors such as pH and ionic strength, and suboptimal binding could have led to loss of protein during the flowthrough phase.[12] Additionally, buffer exchange using an Amicon Ultra Centrifugal Unit may have resulted in minor sample loss, as this step introduces the possibility of protein adhesion to the membrane or inefficient recovery from the filter unit.

A significant yield reduction was observed following TEV protease cleavage. The cleavage reaction was approximately 90% efficient, as evidenced by the presence of both cleaved and uncleaved nsp13 in SDS-PAGE analysis. Therefore, since the cleavage reaction was not 100% effective, some of the uncleaved nsp13 was lost. The secondary IMAC step to remove

TEV protease and uncleaved nsp13 may have removed some of the cleaved protein as well. Although the flowthrough fractions primarily contained cleaved nsp13, the presence of impurities indicates that additional purification was necessary, which can contribute to further loss of protein. The cleaved protein could have still bound to the column, resulting in its loss.

SEC was the final purification step and resulted in a highly purified nsp13 product. However, SEC is known to be a relatively inefficient step in terms of protein recovery. The distinct peak observed in the chromatogram at the expected elution volume confirmed the presence of nsp13, but the overall yield after SEC was significantly reduced to approximately 0.5-1 mg from an initial 4-5 mg post-ion exchange chromatography. Losses during SEC could be attributed to protein aggregation, sample dilution effects, and incomplete recovery of the eluted fractions.[14]

To improve the overall yield, optimization of purification conditions should be considered. One approach is refining buffer compositions to enhance protein stability, solubility, and minimize loss. For example, adjusting pH and salt concentrations in IMAC and ion exchange chromatography can improve binding efficiency and recovery.[34] Additionally, optimizing TEV cleavage conditions by fine-tuning parameters such as enzyme-to-substrate ratio, incubation time, and temperature may enhance cleavage efficiency and reduce the amount of uncleaved protein lost during subsequent purification steps. Another strategy could involve supplementing purification buffers with stabilizing agents such as glycerol or reducing agents to mitigate aggregation or degradation.[34] Also, changing the type of protease inhibitor or adding lysozyme to help break down bacterial cell walls can prevent unwanted degradation.

To further improve yield, optimization strategies should also focus on protein expression. The choice of expression system plays a crucial role in determining final protein yield. Using an optimized *E. coli* strain such as BL21(DE3) pLysS, which reduces basal expression and enhances target protein production, can be beneficial.[1] Additionally, fine-tuning induction conditions, such as adjusting the IPTG concentration or inducing expression at a different temperature, can help reduce protein aggregation and improve protein solubility and stability.[2] In addition, it may be beneficial to have additive such as glycerol that will improve the protein's solubility. The type of growth media used could be changed. Luria-Bertani (LB) is the most used medium and is composed of tryptone, yeast extract, and sodium chloride. While it supports moderate bacterial growth, its relatively low nutrient content may limit biomass accumulation and protein yield. On the other hand, Terrific Broth (TB) is a richer medium, containing additional tryptone, yeast extract, and phosphate buffer, as well as glycerol as an additional carbon source. This composition enhances cell density and prolongs the exponential growth phase, leading to higher protein production. Studies suggest that TB often leads to increased protein expression due to its higher nutrient content and buffering capacity, which prevents excessive acidification during bacterial growth. The higher biomass in TB correlates with greater protein yield, making it preferable for large-scale recombinant protein production. However, excessive protein expression in TB can sometimes lead to protein aggregation or inclusion body formation. LB, while yielding lower protein amounts, may facilitate better solubility due to slower growth and reduced metabolic stress. Therefore, even though LB will result in a lower total yield, it will improve solubility, so more functional protein will be recovered.

3.3 Protein Crystallization

The protein concentration used was 8.8 mg/mL and crystallization trials were performed using the hanging drop vapor diffusion method at 20^{o}C. The optimized condition for crystallizing nsp13 was 0.03 M sodium nitrate, 0.03 M sodium phosphate dibasic, 0.03 M ammonium sulfate, 0.05 M sodium HEPES, 0.05 M MOPS (pH 7.5), 16% ethylene glycol, and 8% PEG 8000. Crystals were observed after a week, and they grew more after a month. Crystal were typically large, spherulitic in shape, and translucent or opaque (Figure 12).

Figure 12. A crystal of nsp13.

Further refinement of crystallization conditions needs to be tested because the crystals diffracted X-rays, but the quality was poor, so nsp13 structure data was not collected. Firstly, protein purity should be checked since impurities can interfere with crystal formation. Different protein concentrations can be tested. Lowering concentration can prevent precipitation while increasing concentration can help promote the formation of crystals. Buffers and pH can be adjusted to ensure the stability of the protein. Precipitant selection also plays an important role in crystal optimization, so alternative precipitants should be tested. Varying the precipitant concentration can help since lowering precipitant concentrations proves to promote slower crystal growth, leading to better-ordered lattices. Temperature is an important factor for crystal growth, so it should also be varied for testing. For example, lower temperatures can reduce protein mobility and enhance ordered lattice growth.

4 CONCLUSION

The worldwide spread of the infectious disease COVID-19 was caused by SARS-CoV-2. An important component to the virus's replication is the nonstructural protein 13 (nsp13). It plays a crucial role in viral replication by unwinding RNA and nsp13 is highly conserved across different coronaviruses, making it a vital target for antiviral drug development. This study focused on optimizing the expression, purification, and crystallization of nsp13 to enhance its structural characterization. By systematically refining each step, significant improvements were achieved, allowing for better protein yield and crystal quality.

This study successfully optimized the expression, purification, and preliminary crystallization of nsp13. By implementing a multi-step purification strategy, purified nsp13 was obtained, demonstrating the effectiveness of the selected methods. The use of IMAC, cation exchange, and size-exclusion chromatography resulted in a pure protein suitable for future structural studies. This study examined various factors influencing the yield and quality of nsp13 protein, from bacterial expression to purification methods and to final crystallization conditions. Through methodical optimization, significant improvements were achieved, demonstrating the importance of fine-tuning each step in the process.

One of the key findings of this research was the effect of expression conditions on protein yield. The study revealed that the choice of the host strain, induction temperature, and inducer concentration had a substantial impact on protein solubility and stability. Lowering the induction temperature and optimizing the IPTG concentration reduced the formation of inclusion bodies, leading to a higher yield of soluble protein.

The purification of nsp13 presented several challenges, particularly in achieving high purity and minimizing loss of protein. Affinity chromatography using a His-tag purification strategy proved effective in isolating nsp13, but additional purification steps such as ion-exchange and size-exclusion chromatography were necessary to remove contaminants. The implementation of an optimized buffer system helped to maintain protein stability, preventing aggregation and degradation. However, more testing needs to be done to increase the solubility and yield of nsp13 so that the overall yield is greater.

Crystallization trials for nsp13 required extensive screening of conditions to identify suitable crystallization parameters. The study found that the hanging-drop vapor diffusion method yielded the most promising crystal formation, with conditions involving polyethylene glycol (PEG) precipitants and divalent cations playing a crucial role in nucleation. The optimization of pH and protein concentration further refined the crystallization process, demonstrating that even minor adjustments could significantly impact crystal quality. The ability to obtain well-ordered crystals is a vital step toward high-resolution structural determination, which is essential for drug-targeting studies. Despite the success, challenges remained, particularly in achieving high-quality crystal formation for X-ray crystallography. Since the structure of nsp13 could not be solved due to poor diffraction, future efforts should focus on optimizing crystallization conditions, including buffer composition, temperature, and protein concentration, to improve crystal diffraction quality.

The findings of this study provide a strong foundation for further structural and functional studies of nsp13. High-quality nsp13 crystals will facilitate X-ray crystallographic analysis, which is crucial for understanding its enzymatic mechanisms and interactions with potential inhibitors. Continued optimization of expression and purification conditions will also benefit other structural studies of SARS-CoV-2 proteins, contributing to broader antiviral research efforts.

In conclusion, this research emphasizes the importance of optimizing each step in the expression, purification, and crystallization of SARS-CoV-2 nsp13. The systematic approach applied in this study led to significant improvements in protein purity and crystallization success, providing a framework for future structural studies. By refining these methodologies, researchers can enhance the efficiency of studying viral proteins, ultimately accelerating drug discovery efforts against SARS-CoV-2 and related coronaviruses. The structural characterization of nsp13 will aid in the rational design of novel therapeutics.

REFERENCES

1. Rosano, G. L.; Ceccarelli, E. A. Recombinant Protein Expression in *Escherichia coli*: Advances and Challenges. *Front. Microbiol.* **2014**, *5*, 1–17. https://doi.org/10.3389/fmicb.2014.00172
2. Liu, L., Yang, H., Shin, H., Chen, R. R., Li, J., & Du, G. How to achieve high-level expression of microbial enzymes: Strategies and perspectives. *Bioengineered*, ***2013,*** *4*(4), 212-223. https://doi.org/10.4161/bioe.24761
3. Kimple, M. E.; Brill, A. L.; Pasker, R. L. Overview of Affinity Tags for Protein Purification. *Curr. Protoc. Protein Sci.* **2013**, *73* (1), 9.9.1–9.9.23. https://doi.org/10.1002/0471140864.ps0909s73.
4. Bornhorst, J. A.; Falke, J. J. Purification of Proteins Using Polyhistidine Affinity Tags. *Methods Enzymol.* **2000**, *326*, 245–254. https://doi.org/10.1016/S0076-6879(00)26058-8.
5. Gaberc-Porekar, V.; Menart, V. Potential for Using Histidine Tags in Purification of Proteins at Large Scale. *Chem. Eng. Technol.* **2005**, *28* (11), 1306–1314. https://doi.org/10.1002/ceat.200500167.
6. Polayes, D. A.; Parks, T. D.; Johnston, S. A.; Dougherty, W. G. Application of TEV Protease in Protein Production. *Methods Mol. Med.* **1998**, *13*, 169–183. https://doi.org/10.1385/0-89603-485-2:169.
7. Urh, M.; Simpson, D.; Zhao, K. Affinity Chromatography: General Methods. *Methods Enzymol.* **2009**, *463*, 417–438. https://doi.org/10.1016/S0076-6879(09)63026-3
8. Block, H.; Maertens, B.; Spriestersbach, A.; Brinker, N.; Kubicek, J.; Fabis, R.; Labahn, J.; Schäfer, F. Immobilized-Metal Affinity Chromatography (IMAC): A Review. *Methods Enzymol.* **2009**, *463*, 439–473. https://doi.org/10.1016/S0076-6879(09)63027-5.

9. Riguero, V.; Clifford, R.; Dawley, M.; Dickson, M.; Gastfriend, B.; Thompson, C.; Wang, S.-C.; O'Connor, E. Immobilized Metal Affinity Chromatography Optimization for Poly-Histidine Tagged Proteins. *J. Chromatogr. A* **2020**, *1629*. https://doi.org/10.1016/j.chroma.2020.461505.
10. **Arnau, J.; Lauritzen, C.; Petersen, G. E.; Pedersen, J.** Current Strategies for the Use of Affinity Tags and Tag Removal for the Purification of Recombinant Proteins. *Protein Expr. Purif.* **2006**, *48* (1), 1–13. https://doi.org/10.1016/j.pep.2005.12.002.
11. Jungbauer, A.; Hahn, R. **Ion-Exchange Chromatography.** *Methods Enzymol.* **2009**, *463*, 349–371. https://doi.org/10.1016/S0076-6879(09)63022-6.
12. Cummins, P. M.; Rochfort, K. D.; O'Connor, B. F. Ion-Exchange Chromatography: Basic Principles and Application. In *Protein Chromatography*; Springer, 2016; pp 209–223. https://doi.org/10.1007/978-1-4939-6412-3_11.
13. Barth, H. G.; Boyes, B. E.; Jackson, C. Size exclusion chromatography. *Anal. Chem.* **1994**, *66*, 595R–620R.
14. Sun, T.; Chance, R. R.; Graessley, W. W.; Lohse, D. J. A Study of the Separation Principle in Size Exclusion Chromatography. *Macromolecules* **2004**, *37*(11), 4304–4312. https://doi.org/10.1021/ma030586k.
15. Brunelle, J. L.; Green, R. One-Dimensional SDS-Polyacrylamide Gel Electrophoresis (1D SDS-PAGE). *Methods Enzymol.* **2014**, *541*, 151–159. https://doi.org/10.1016/B978-0-12-420119-4.00012-4.
16. Manns, J. M. SDS-Polyacrylamide Gel Electrophoresis (SDS-PAGE) of Proteins. *Curr. Protoc. Microbiol.* **2011**, *22*, A.3M.1–A.3M.13. https://doi.org/10.1002/9780471729259.mca03ms22.

17. McPherson, A. Introduction to Protein Crystallization. *Methods* **2004**, *34*(3), 254–265. https://doi.org/10.1016/j.ymeth.2004.03.019.

18. Durbin, S. D.; Feher, G. Protein Crystallization. *Annu. Rev. Phys. Chem.* **1996**, *47*, 171–204. https://doi.org/10.1146/annurev.physchem.47.1.171.

19. Weber, P. C. Physical Principles of Protein Crystallization. *Adv. Protein Chem.* **1991**, *41*, 1–36. https://doi.org/10.1016/S0065-3233(08)60196-5.

20. Ducruix, A., & Giegé, R. (Eds.). (1999). *Crystallization of nucleic acids and proteins: A practical approach*. Oxford University Press.

21. Hou, H.; Shi, M.; Hu, S.-Y.; Ahmad, F.; Zhang, B.; Chen, Z.-H.; Yin, D.-C. A Systematic Comparison of Sitting and Hanging-Drop Crystallization Using Traditional and Cross-Diffusion Microbatch Crystallization Plates. *J. Cryst. Growth* **2019**, *521*, 1–8. https://doi.org/10.1016/j.jcrysgro.2019.05.011.

22. McPherson, A. Protein Crystallization. In *Protein Crystallography*; Wlodawer, A., Dauter, Z., Jaskolski, M., Eds.; Methods in Molecular Biology, Vol. 1607; Humana Press: New York, NY, 2017; pp 17–50. https://doi.org/10.1007/978-1-4939-7000-1_2.

23. Ducruix, A., & Giegé, R. (Eds.). (1999). *Crystallization of nucleic acids and proteins: A practical approach*. Oxford University Press.

24. Shi, Y.; Wang, G.; Cai, X.-P.; Deng, J.-W.; Zheng, L.; Zhu, H.-H.; Zheng, M.; Yang, B.; Chen, Z. An overview of COVID-19. *J. Zhejiang Univ., Sci. B* **2020**, *21* (5), 343–360. https://doi.org/10.1631/jzus.B2000083.

25. Ciotti, M.; Ciccozzi, M.; Terrinoni, A.; Jiang, W.-C.; Wang, C.-B.; Bernardini, S. The COVID-19 Pandemic. *Crit. Rev. Clin. Lab. Sci.* **2020**, *57* (6), 365–388. https://doi.org/10.1080/10408363.2020.1783198.

26. Saif, L. J.; Wang, Q.; Vlasova, A. N.; Jung, K.; Xiao, S. Coronaviruses. In *Diseases of Swine*; Zimmerman, J. J., Karriker, L. A., Ramirez, A., Schwartz, K. J., Stevenson, G. W., Zhang, J., Eds.; Wiley, 2019. https://doi.org/10.1002/9781119350927.ch31.

27. Weiss, S. R.; Leibowitz, J. L. Coronavirus Pathogenesis. *Adv. Virus Res.* **2011**, *81*, 85–164. https://doi.org/10.1016/B978-0-12-385885-6.00009-2.

28. Yadav, R.; Chaudhary, J. K.; Jain, N.; Chaudhary, P. K.; Khanra, S.; Dhamija, P.; Sharma, A.; Kumar, A.; Handu, S. Role of Structural and Non-Structural Proteins and Therapeutic Targets of SARS-CoV-2 for COVID-19. *Cells* **2021**, *10* (4), 821. https://doi.org/10.3390/cells10040821.

29. Newman, J. A.; Douangamath, A.; Yadzani, S.; Yosaatmadja, Y.; Aimon, A.; Brandao-Neto, J.; Dunnett, L.; Gorrie-Stone, T.; Skyner, R.; Fearon, D.; Schapira, M.; von Delft, F.; Gileadi, O. Structure, Mechanism, and Crystallographic Fragment Screening of the SARS-CoV-2 NSP13 Helicase. *Nat. Commun.* **2021**, *12*. https://doi.org/10.1038/s41467-021-25166-6.

30. Yue, K.; Yao, B.; Shi, Y.; Yang, Y.; Qian, Z.; Ci, Y.; Shi, L. The Stalk Domain of SARS-CoV-2 NSP13 Is Essential for Its Helicase Activity. *Biochem. Biophys. Res. Commun.* **2022**, *601*, 129–136. https://doi.org/10.1016/j.bbrc.2022.02.068.

31. Grimes, S. L.; Denison, M. R. The Coronavirus Helicase in Replication. *Virus Res.* **2024**, *346*, 199401. https://doi.org/10.1016/j.virusres.2024.199401.

32. Ivanov, K. A.; Thiel, V.; Dobbe, J. C.; van der Meer, Y.; Snijder, E. J.; Ziebuhr, J. Multiple Enzymatic Activities Associated with Severe Acute Respiratory Syndrome Coronavirus Helicase. *J. Virol.* **2004**, *78*(11), 5619–5632. https://doi.org/10.1128/jvi.78.11.5619-5632.2004

33. Zeng, J.; Weissmann, F.; Bertolin, A. P.; Posse, V.; Canal, B.; Ulferts, R.; Wu, M.; Harvey, R.; Hussain, S.; Milligan, J. C.; Roustan, C.; Borg, A.; McCoy, L.; Drury, L. S.; Kjaer, S.; McCauley, J.; Howell, M.; Beale, R.; Diffley, J. F. X. Identifying SARS-CoV-2 Antiviral Compounds by Screening for Small Molecule Inhibitors of nsp13 Helicase. *Biochem. J.* **2021**, *478*(13), 2405–2423. https://doi.org/10.1042/BCJ20210201.

34. Che Hussian, C. H. A.; Leong, W. Y. Factors Affecting Therapeutic Protein Purity and Yield During Chromatographic Purification. *Prep. Biochem. Biotechnol.* **2024**, *54*(2), 150–158. https://doi.org/10.1080/10826068.2023.2217507